



An insertional trap for conditional gene expression in *Toxoplasma gondii*: Identification of TAF250 as an essential gene

Lauren Jammallo^{a,1}, Keith Eidell^{a,1}, Paul H. Davis^{b,2}, Fay J. Dufort^a, Courtney Cronin^a, Sivasakthivel Thirugnanam^a, Thomas C. Chiles^a, David S. Roos^b, Marc-Jan Gubbels^{a,*}

^a Department of Biology, Boston College, 140 Commonwealth Ave., Chestnut Hill, MA, United States

^b Department of Biology and Penn Genomics Institute, University of Pennsylvania, Philadelphia, PA, United States

ARTICLE INFO

Article history:

Received 25 August 2010

Received in revised form 18 October 2010

Accepted 19 October 2010

Available online 28 October 2010

Keywords:

Toxoplasma gondii

Invasion

Cell cycle

TAF250

Chaperonin

Genetic screen

ABSTRACT

Toxoplasmosis is characterized by fast lytic replication cycles leading to severe tissue lesions. Successful host cell invasion is essential for pathogenesis. The division cycle of *Toxoplasma gondii* is characterized by an unusual cell cycle progression and a distinct internal budding mechanism. To identify essential genes involved in the lytic cycle we devised an insertional gene trapping strategy using the Tet-transactivator system. In essence, a random, active promoter is displaced with a tetracycline regulatable promoter, which if in an essential gene, will result in a conditionally lethal phenotype upon tetracycline addition. We isolated eight mutants with growth defects, two of which displayed modest invasion defects, one of which had an additional cell cycle defect. The trapped loci were identified using expression microarrays, exploiting the tetracycline dependent expression of the trapped genes. In mutant 3.3H6 we identified TCP-1, a component of the chaperonin protein folding machinery under the control of the Tet promoter. However, this gene was not critical for growth of mutant 3.3H6. Subsequently, we identified a suppressor gene encoding a protein with a hypothetical function by guided cosmid complementation. In mutant 4.3B13, we identified TAF250, an RNA polymerase II complex component, as the trapped, essential gene. Furthermore, by mapping the plasmid insertion boundaries we identified multiple genomic rearrangements, which hint at a potential replication dependent DNA repair mechanism. Furthermore, these rearrangements provide an explanation for inconsistent locus rescue results observed by molecular biological approaches. Taken together, we have added an approach to identify and study essential genes in *Toxoplasma*.

© 2010 Elsevier B.V. All rights reserved.

1. Introduction

Infection with the apicomplexan parasite *Toxoplasma gondii* is associated with severe disease in immunocompromised patients and with a variety of birth defects when infection is contracted congenitally. Clinical toxoplasmosis is characterized by the acute or reemerging fast-replicating tachyzoite life stage, which is defined by lytic infection rounds destroying cells of the host in the process [1]. The mechanics of the intracellular division process are dramatically different from the mammalian host, however the ultimate cell cycle progression control mechanisms are similar to those found in all eukaryotes [2–4].

The critical components in the division process have been difficult to study in these haploid organisms because inactivation of these genes results in lethal phenotypes. However, in recent years several approaches have been developed to study essential genes in *T. gondii*. Most of these require candidate gene approaches, where a gene of interest is cloned in a conditional expression system, either on the transcriptional level using the Tet-transactivator [5] or Tet-repressor system [6,7], or at the post-translational level using a small molecule to stabilize a destabilization domain to regulate proteasomal turnover [8]. On the other hand, random mutagenesis to generate temperature sensitive mutants in which the mutated gene is subsequently identified through wild-type genetic cosmid complementation allows the unbiased identification of essential genes [9]. Stage specific essential genes have been successfully studied by insertional mutagenesis based signature mutagenesis [10]. In this study we set out to combine the strengths from conditional expression of candidate genes with the unbiased approach of insertional mutagenesis.

The approach we followed exploits the high random integration frequency while directing the insertion event by a promoter

* Corresponding author. Tel.: +1 617 552 8722; fax: +1 617 552 2011.

E-mail address: gubbelsj@bc.edu (M.-J. Gubbels).

¹ These authors contributed equally.

² Present address: Department of Biology, University of Nebraska-Omaha, United States.

trap with a drug-selectable marker, simultaneously resulting in replacement of the promoter of the trapped gene with a conditional Tet-transactivator promoter. As such, if an essential gene is trapped, the addition of anhydrotetracycline (ATc) will result in down regulation of gene expression and produce a conditionally lethal phenotype. Several conditional mutants were isolated with tachyzoite growth defects using this conditional trapping method. Two mutants were analyzed in greater detail. To identify the trapped genes we identified differentially expressed genes upon ATc addition using the Affymetrix GeneChip available for *T. gondii*. For both mutants we successfully identified the trapped and conditionally expressed genes, although only in one case the locus responsible for growth arrest could be confirmed. Taken together, the methodology described here combines various recently developed technologies and adds an additional tool to identify and study essential genes in *T. gondii*.

2. Materials and methods

2.1. Parasites

RH strain parasites and transgenic derivatives were used throughout this study. Parasites were maintained in human foreskin fibroblasts as previously described [11]. Transactivator expressing parasites, the Ta-Ti strain, were kindly provided by Dominique Soldati [5]. Additionally, the Ta-Ti strain was stably transfected with plasmid ptubYFP₂/sagCAT [12] and cloned by limiting dilution to produce the Ta-Ti-YFP2 parent line.

2.2. Plasmids

All primer sequences are provided in supplementary Table S1. Plasmid tub-H2b-mRFP/sagCAT has been described previously [13]. Plasmid DHFRtet7sag4-SpeI was constructed by PCR amplification of the Tet7sag4 promoter [5] using the primers TetSag4Xba and TetSag4Not and cloned *XbaI/NotI* into plasmid pDHFR-TSC3ABP [14]. Subsequently, plasmid Tet7sag4DHFR-Sfi was cloned by PCR amplification of the DHFR ORF using primers DHFR-ORF-for and DHFR-3UTR-Asc and cloning *XbaI/PacI* into pDHFRtet7sag4-SpeI. Next, plasmid Tet7sag4DHFR-Xba-Kan was cloned by pDONR2.1 digestion with *AvaI* and *PstI* and T4 DNA polymerase end-filling. Tet7sag4DHFR-Sfi was digested with *NotI/PacI/ScaI* and the ends were filled and both fragments blunt-end ligated. Subsequently, plasmid Tet7sag4-HX3UTR-DHFR-Xba-Kan was cloned by PCR amplification of the HXGPRT 3'UTR with *XhoI* and *XbaI* flanking primers HX-3UTR-XX-F and HX-3UTR-Xba-R and cloned *XbaI* in Tet7sag4DHFR-Xba-Kan. Finally, plasmid Tet7sag4-HX3UTR-3STOP-DHFR-Xba-Kan was cloned by PCR amplification of the HXGPRT 3'UTR from Tet7sag4-HX3UTR-DHFR-Xba-Kan using primers HX-3UTR-XX-F and 3xSTOP-UTR-AgeI; the amplicon was cloned *NdeI/AgeI* into the parent plasmid.

Plasmid ptub-TCP1-YFP/sagCAT was cloned by PCR amplification of TCP-1 from 77.m00088 using primers TCP-1-BglII-F and TCP-1-AvrII-R; the amplicon was cloned *BglII/AvrII* into the ptub-YFP₂(MCS)/sagCAT plasmid.

Plasmid ptub-YFP-TCP1/sagCAT was cloned by PCR amplification of TCP-1 from 77.m00088 using primers TCP-1-AvrII-F and TCP-1-SmaI-R. The amplicon was cloned *AvrII/XmaI* into the ptub-YFP₂(MCS)/sagCAT plasmid.

Plasmid ptub-72.m00683-YFP/sagCAT was cloned by PCR amplification of the 72.m00683 ORF from cDNA using primers 72.m000683BglIIF and 72.m000683AvrIIR. The amplicon was cloned *BglII/AvrII* into the ptub-YFP₂(MCS)/sagCAT plasmid.

Plasmid ptub-YFP-72.m00683/sagCAT was cloned by PCR amplification of the 72.m00683 ORF from cDNA using primers

72.m000683AvrIIF and 72.m000683EvoRVR; the amplicon was cloned *AvrII/EcoRV* into the ptub-YFP₂(MCS)/sagCAT plasmid.

2.3. Insertional mutagenesis and growth mutant screen

For insertional mutagenesis 50 µg of plasmid DNA was digested with the selected restriction enzymes and gel purified. Transfected Ta-Ti-YFP2 parasites were selected for pyrimethamine resistance. Parallel plaque assays were set up immediately following mutagenesis under the following selective conditions: no selection (control), 1 µg/ml anhydrotetracycline (ATc; Clontech, Mountain View, CA), 1 µM pyrimethamine and finally the combination of ATc and pyrimethamine. To isolate ATc conditional clones, the polyclonal population was seeded in 384-well plates confluent with HFF cells at a concentration of 3 parasites per well [9]. After parasite growth for 7 days, plates were duplicated using a 5 µl pintoole as previously described into plates with optical bottom with 1 µg/ml ATc and a plate without ATc in medium lacking phenol red [9]. After growth for 6 days, YFP fluorescence increase corresponding with parasite growth was read on a BMG Fluostar plate reader as previously described [12]. Corresponding wells displaying growth without ATc, but with no YFP increase in the plate with ATc, were picked and re-screened visually for ATc conditional growth in 24-well plates. Positive parasite clones were picked for further study.

2.4. Growth curves

Parasite growth curves based on cytoplasmically expressed YFP were recorded in 384-well plates in quadruplicate as described previously [9,12]. Fluorescence was read daily with a Molecular Dynamics M5 plate reader using 510 nm excitation and 540 nm emission wavelength settings using a 530 nm cut off.

2.5. Invasion assays

Invasion efficiency was evaluated using the method described by Carey et al. [15]. Briefly, parasites were grown for 30, 36 or 48 h in the presence of 1 µg/ml ATc (or vehicle control) and mechanically released from the host cell by passage through a 26.5 G needle. Parasites were incubated for 1 h with HFF cells grown in 96-well plates at 37 °C. Extracellular parasites were identified by immunofluorescence using mAb T51E5 (kindly provided by Dr. Jean François Dubremetz) followed by Alexa594-conjugated goat anti-mouse IgG (Molecular Probes).

2.6. DNA content analysis

The cell cycle stage was determined using methods described previously to determine DNA content [9,16]. Parasites were syringed from the host cells and filtered through a 12 µm carbonate filter to include large, polyploid parasites in the analysis. A FACSCanto cytometer (BD Franklin Lakes, NJ) was used and 50,000 events were collected. Data were prepared for publication using FlowJo software by gating for the parasite population based on side scatter (SSC) and fluorescence intensity (Treestar, Ashland, OR).

2.7. Immunofluorescence

IFAs were performed as described previously [13]. The following primary antibodies were used: rat α-IMC3 [17] and human α-Centrin (kindly provided by Dr. Iain Cheeseman, Whitehead Institute). DNA was stained with 4',6-diamidino-2-phenylindole (DAPI). Secondary goat-raised antibodies were Alexa488 or Alexa594 conjugated (Invitrogen/Molecular Probes). Images were collected on a Zeiss Axiovert 200M wide-field fluorescence microscope equipped with standard DAPI, FITC and TRITC filter sets, a

NEOFLUAR 100 \times /1.3 objective and a Hamamatsu C4742-95 CCD camera. Images were acquired and processed for presentation using Volocity Software (Improvision/Perkin Elmer, Coventry, UK).

2.8. Microarrays and analysis

The parent line and mutants were grown for 33 h at 37 °C with and without 1 μ g/ml ATc, mechanically released by needle passage and washed twice with PBS by centrifugation at 24 °C, 1000 \times g for 15 min. Total RNA was extracted with Trizol (Invitrogen), resuspended in DEPC treated water and treated with DNase (Ambion). Total RNA samples were stored at –80 °C in the presence of RNase inhibitor until further use. 100 ng of total RNA was converted into first-strand cDNA using reverse transcriptase primed by a poly(T) oligomer incorporating a synthetic RNA sequence. Second-strand cDNA synthesis was followed by ribo-SPIA (Single Primer Isothermal Amplification, NuGEN Technologies Inc., San Carlo, CA) for linear amplification of each transcript. 4 μ g of the resulting cDNA was fragmented using the standard NuGen process, assessed by Bioanalyzer, and biotinylated. Biotin-labeled cDNAs were added to Affymetrix hybridization cocktails, heated at 99 °C for 2 min and hybridized for 16 h at 45 °C with the GeneChips (Affymetrix Inc., Santa Clara, CA) [18]. An Affymetrix GeneChip Scanner 3000 7G confocal scanner was used to collect fluorescence signal after excitation at 570 nm. Affymetrix Command Console v2 software was used to determine raw intensities and generate CEL files. Default values provided by Affymetrix were applied to all analysis parameters; border pixels were removed, and the average intensity of pixels within the 75th percentile was computed for each probe. The average of the lowest 2% of probe intensities occurring in each of 16 microarray sectors was set as background and subtracted from all features in that sector. Global scaling was applied to allow comparison of gene signals across multiple microarrays. RMAExpress v1.00 was used to compute gene expression summary values for Affymetrix data using the Robust Multichip Average expression summary.

2.9. Mapping of the insertional breakpoints

To map the insertional breakpoint in locus 77.m00088 at the 3'-end of the inserting plasmid we used primer Tet07Sag4-F encoded in the plasmid Tet7sag4 promoter over the *Hind*III site and primer 77.m00088R1, which amplified 490 bp. We also used Tet07Sag4-F in combination with primer 77.m00088R2, which amplified a 970 bp product. To map the insertional breakpoint at the 5'-end of the inserting plasmid we used primer Tet07Sag4-R (localized within the DHFR ORF) and primer 77.m00088-F to amplify a 1.2 kb fragment. To map the insertional breakpoint in locus 64.m00349 at the 3'-end of the inserting plasmid we used primer Tet07Sag4-F and primer #5-set1R644.3, which amplified a 1360 bp product. To map the insertional breakpoint at the 5'-end of the inserting plasmid, we used primers #5-set1F644.3 and Tet07Sag4-R to amplify a 2372 bp fragment. Sequencing reactions of TOPO cloned PCR products were performed by Operon (Huntsville, AL).

2.10. qRT-PCR

TCP-1 (77.m00088) was amplified using primers qRTPCR-77.m00088-F and qRTPCR-77.m00088-R; 149 bp were amplified. The housekeeping gene, actin (25.m00007), was amplified using primers qRTPCR-Actin-F, qRTPCR-Actin-R. The housekeeping gene GAPDH (80.m00003) was amplified using primers qRTPCR-GAPDH-F and qRTPCR-GAPDH-R. RNA was isolated using Trizol at 33 h for mutant 3.3H6 and parent with and without ATc. cDNA was synthesized using the iScript cDNA Synthesis Kit (Bio-Rad Laboratories).

SYBR Green PCR Master Mix (2 \times) (Bio-Rad) was used for qRT-PCR. A 96-well PCR plate (Bio-Rad) was used and the reaction was run on a Realplex Thermocycler (Eppendorf). Data were analyzed using the Realplex software (Eppendorf).

2.11. Southern blotting

Southern blotting was performed as described in Ref. [14]. Genomic DNA was digested with the following restriction enzymes: *Bgl*III, *Xmn*I or *Age*I. Three probes were generated by PCR, a Kan-probe (Kan-F and Kan-R primers; 675 bp), a 5'-TCP-1 probe (5'-TCP1-F and 5'-TCP1-R primers; 552 bp) and a 3'-TCP-1 probe (3'-TCP1-F and 3'-TCP1-R primers; 543 bp). Probes were radioactively labeled with α -[³²P]-dATP by random primer labeling (Invitrogen).

2.12. Cosmid complementation

Cosmids TOX0867 spanning gene 77.m00088 and cosmid TOX0178 spanning gene 64.m00349 were grown up and purified from the arrayed cosmid library as described previously [2]. The following cosmids were used for complementation efforts of mutant 3.3H6: TOX0867 for gene 77.m00088, PSBLV88, PSBM403, and PSBM924 for gene 72.m00683, TOXPG21 for gene 641.m02543, TOXOE28 for gene 83.m01259, and TOX0854 for gene 50.m03365. Complementation experiments were performed in duplicate in independent experiments using an unrelated cosmid as a negative control.

2.13. Phylogenetic analysis

TAF250 orthologs from the following species, including database accession numbers, were used for phylogenetic analysis: *Neospora caninum*, NCLIV_006970; *Plasmodium falciparum*, PFL1645w; *Plasmodium knowlesi*, PKH_145120; *Theileria annulata*, XP_954404.1; *Babesia bovis*, XP_001610355.1; *Cryptosporidium parvum*, XP_625669.1; *Arabidopsis thaliana*, NP_174552.1; *Oryza sativa*, Q67W65.1; *Danio rerio*, NP_001038250.1; *Caenorhabditis elegans*, NP_493426.2; *Mus musculus*, Q80UV9.2; *Homo sapiens*, EAX05291.1. Sequences were aligned using default setting on ClustalW [19] and analyzed by the neighbor-joining and bootstrap analysis algorithms in the MEGA4 software package [20].

3. Results

3.1. Conditional gene trapping by insertional mutagenesis

The strategy to generate conditional mutants by trapping essential genes under the control of the tetracycline inducible promoter, Tet7sag4, using the Tet-off system is outlined in Fig. 1. The parasite line (Ta-Ti-YFP2) used for insertional mutagenesis with the trapping plasmid already expresses the Tet-dependent transactivator [5]. In addition, this parasite line was stably transfected with a cytoplasmic, tandem YFP expressing plasmid, which enables automated screening for growth mutants using the increase in cytoplasmic YFP fluorescence as a read-out for parasite growth [9,12]. We designed an insertional trapping plasmid that, upon linearization with restriction enzymes, on the 5'-end harbors a promoterless DHFR-TSm2m3 gene endowing resistance to pyrimethamine and on the 3'-end a Tet7sag4 promoter (Fig. 1A). Exploiting the high frequency of random genomic integration of plasmid DNA transfected into the parasite [21], an insertion in a gene between the promoter and the start codon would result in a pyrimethamine resistant parasite with the trapped gene conditional upon ATc addition. Consequently, only trapping of essential genes will result in conditionally lethal phenotypes.

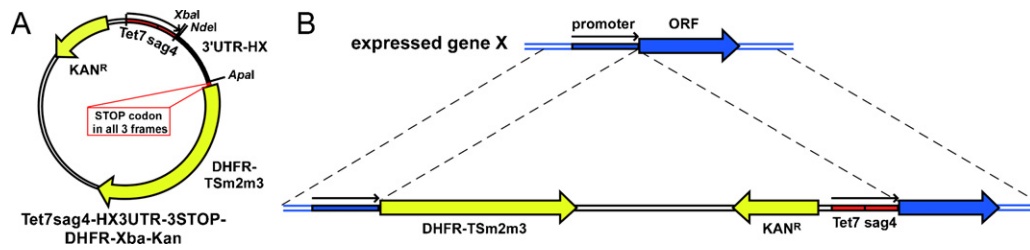


Fig. 1. Schematic outline of insertional trapping with the Tet7sag4 conditional promoter. (A) Map of trapping plasmid. The plasmid is 5351 bp long, whereas the *Apal*/*NdeI* restriction site flanked linker is 439 bp long. (B) Strategy of mutant generation. The 3'UTR terminator of HXGPR1 is removed before transfection by restriction digestion with *NdeI* and *Apal* and purified by gel electrophoresis. To avoid in-fusion insertion in introns, the DHFR ORF is preceded by stop-codons in the three reading frames.

3.2. Identification of growth mutants

As described above, linearized trapping plasmid was transfected into the Ta-Ti-YFP2 parasite line to randomly trap promoters. Upon selection for stable pyrimethamine resistance, the parasite population was seeded into 384-well plates at a density of 3 parasites per well. Parasites in plates were grown up for a week and then replica-plated into one plate with and one plate without ATc. Following growth for 6 days, wells containing conditional mutants were identified using the cytoplasmically expressed YFP as a measure for parasite growth. In total, we isolated 8 mutants with the desired conditional phenotype from four independent transfections (a total of forty 384-well plates was screened). Mutants isolated from the same transfection were considered independent when their growth kinetics showed different profiles. Growth curves of three representative mutants and the parent line are shown in Fig. 2. Most mutants shut down completely in the presence of ATc (e.g. independent mutants 3.3H6 and 4.3B13), whereas other mutants displayed a reduced growth (e.g. mutant 3.3G21, which was isolated from the same mutagenesis as mutant 3.3H6). Importantly, none of these mutants are conditionally resistant to pyrimethamine, indicating the insertional event took place such that the promoter of the trapped gene drives DHFR-TSm2m3 expression and the Tet7sag4 promoter drives expression of the trapped gene.

3.3. Phenotypic analysis

Since growth defects can be due either to an intracellular development defect or to defects in host cell invasion, we tested these two different aspects. First we determined the potential defects in host cell invasion employing the 'red-green' invasion assay [15]. Fig. 3A shows that after 24 h in the presence of ATc (phenotype induced) the host cell invasion capacity of mutants 3.3H6 and 4.3B13 is strongly inhibited compared to the wild-type parent line: 56% and 29% of the parasites remain extracellular, respectively, compared to only 11% of the parent parasites. None of the other mutants displayed a reduction in invasion efficiency compared to the wild-type (data not shown). For these two apparent invasion

mutants we additionally determined whether or not these mutants displayed a cell cycle defect. This was measured by DNA content analysis using flow cytometry after various times of ATc induction. The parent line displayed the typical cell cycle distribution pattern for randomly cycling parasites (Fig. 3B) [9,22]. Note that the population with a DNA content with more than 2N is due to using a large filter pore size (12 μm) in preparation of the samples and the relaxed gating to enable detection of large, polyploid parasites. These results are comparable to a previous study [16]. For mutant 3.3H6, upon ATc incubation an increasing population with nuclear contents larger than 2N was observed (Fig. 3C). Such a profile suggests the development of an uncoupling phenotype wherein DNA replication progresses in the absence of cell division [2,9,16]. To validate this assessment we analyzed the parasites by immunofluorescence using two markers for intracellular development; IMC3, which outlines the cortical cytoskeleton of the parasite and additionally marks the internally budding daughter cytoskeletons, and an antibody marker for the centrosome, which duplicates at the start of S-phase [23] (Fig. 3E). As expected, in addition to normal appearing parasites (Fig. 3F) we observed the appearance of parasites with larger than normal nuclei associated with more than 2 centrosomes in the absence of internal budding, which is consistent with the uncoupling phenotype (Fig. 3G and H). For mutant 4.3B13 the DNA content profiles at all time points reflected the parent line (Fig. 3D). Analysis of the parasites by immunofluorescence did not identify any defects in parasite morphology or daughter budding (Fig. 3I). However, it is possible that specific defects could be detected by studying other phenotypic features. Together with the growth kinetics (Fig. 2C), these data indicate that mutant 4.3B13 growth arrests between 36 and 48 h after addition of ATc which can occur at any stage randomly in the cell cycle without obvious morphological changes.

3.4. Gene 77.m00088, encoding a TCP1 chaperonin component, is trapped and conditionally expressed in mutant 3.3H6

We reasoned that mapping the locus trapped by the inserting plasmid could be identified using the Affymetrix *T. gondii* genechip

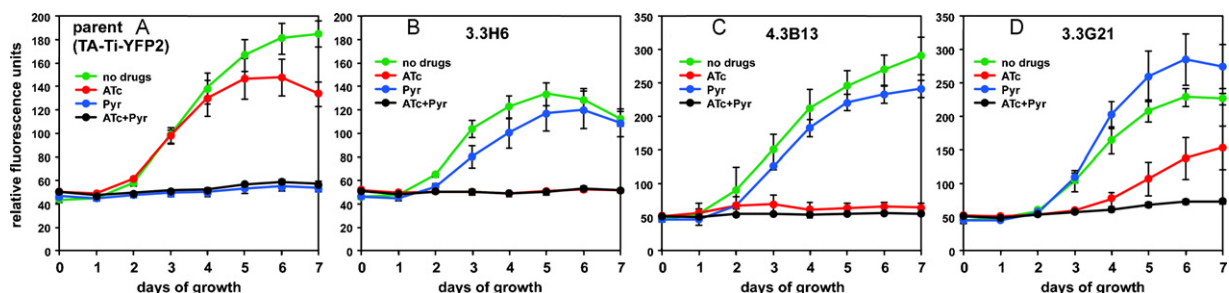


Fig. 2. Growth kinetics of representative mutants. Growth curves of the parent line (A) and mutants 3.3H6 (B), 4.3B13 (C) and 3.3G21 (D) under various drug pressures. Mutants enter growth arrest when ATc is in the medium, whereas the parent line grows undisturbed. Cytoplasmically expressed tandem YFP was used as a daily read-out in a 384-well plate assay [12]. Error bars denote standard deviation of four replicates.

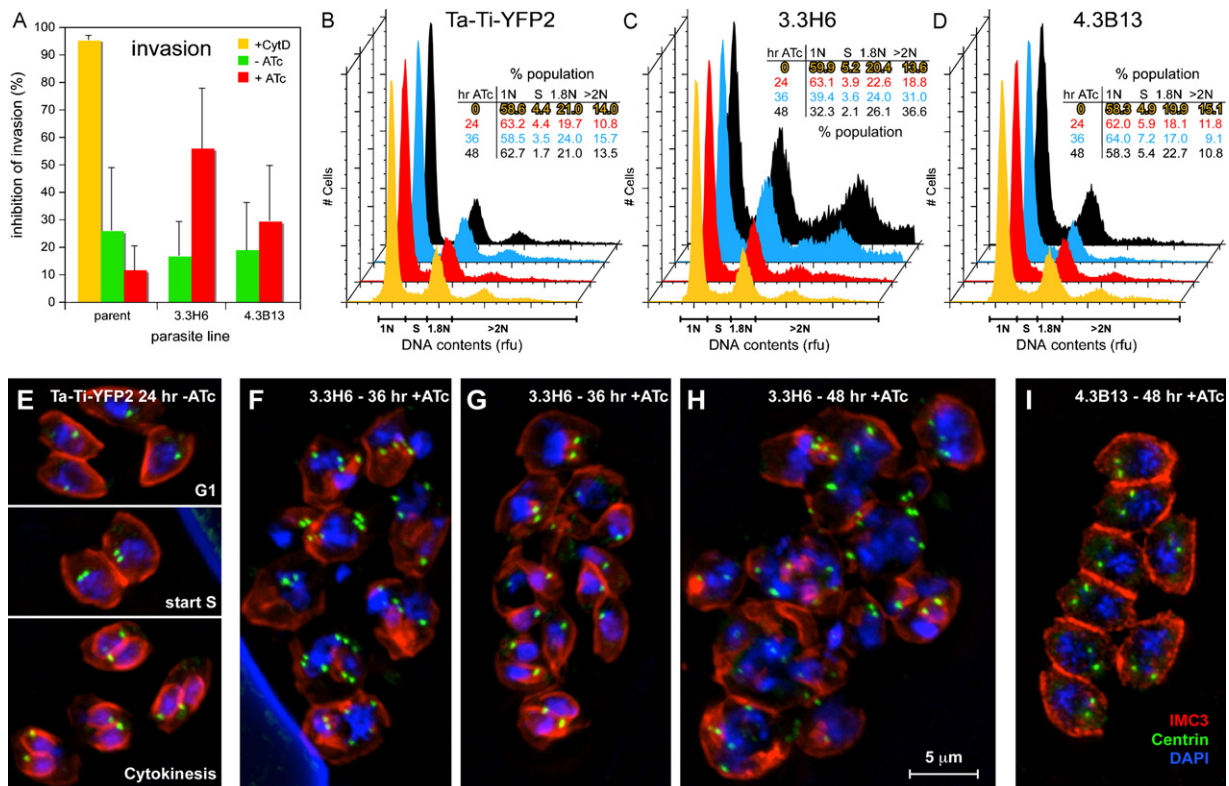


Fig. 3. Phenotypic characterization of growth arrest of mutants 3.3H6 and 4.3B13. (A) Invasion assays of parent and mutants in absence and presence of ATc induction for 48 h. Cytochalasin D (CytD) is used as an efficient invasion blocking control. Assay essentially as in Ref. [15]. Error bars denote standard deviation of three replicates. (B–D) Flow cytometry analysis of DNA content of the parent line (B) and mutants 3.3H6 (C) and 4.3B13 (D). Profiles after 0, 24, 36 and 48 h of ATc induction are shown in yellow, red, blue and black, respectively. Inserted tables display the population development of the various cell cycle stages as a function of ATc induction time. Population definitions are indicated along the x-axis; rfu denotes relative area fluorescence units. (E–I) Immunofluorescence assays with α -IMC3 and α -centrin co-stained with DAPI for 3.3H6 and 4.3B13 at various time points with and without ATc induction as indicated. (For interpretation of the references to color in this figure legend, the reader is referred to the web version of the article.)

array since expression of the trapped gene is expected to shut down upon addition of ATc [18]. Therefore, we collected total RNA from the parent and mutant parasite lines grown in either the absence or presence of ATc for 33 h to allow reduction of the transcript and hybridized these samples to the genechip array. Only one gene in the parent line expressed an over 2-fold difference in intensity upon ATc addition: a 2.13-fold reduction for gene 148.m00016, which encodes a DNA polymerase (Fig. S1). For mutant 3.3H6 gene 77.m00088 displayed a 12-fold repression upon ATc (Fig. 4A–C), with the next best candidate (gene 642.m00040) only displaying 2.9-fold suppression (Fig. 4B). We independently validated the conditional expression of gene 77.m00088 at the same incubation time with ATc (33 h) for both parent and mutant by qRT-PCR. In the parent line the expression level of gene 77.m00088 was 1.6-fold higher by gene-chip and 2-fold higher by qRT-PCR (Fig. 4C and D). In mutant 3.3H6 we detected a 15-fold down-regulation by qRT-PCR (Fig. 4D), which closely matches and validates the gene-chip data (12-fold).

To demonstrate that the observed differential expression is indeed due to integration of the conditional promoter trap plasmid we mapped the genomic insertion site. Since the trapping method is designed to insert directly in front of the start codon, we designed a sense primer hybridizing to the Tet7sag4 promoter and two different anti-sense primers 300 bp apart, one in the promoter and one right behind the start codon. Using the anti-sense primer in the promoter we successfully amplified a 490 bp product spanning the 3'-breakpoint in gene 77.m00088 (Fig. 4E). A similar approach was taken to PCR amplify the 5'-end of the insertion site. When 5'- and 3'-end breakpoints were mapped onto the chromosome a clean break without a single nucleotide loss was mapped. On the

plasmid side of the insertion 2 nucleotides were lost on the 3'-end of the *NdeI* site (Fig. 4E). The 5'-end of the plasmid clearly identified the beginning of the DHFR-TS open reading frame including two remaining base pairs of the *Apal* site. However, an additional stretch of 303 bp was identified, which corresponded with three different fragments of the trapping plasmid: the first 143 bp corresponding with the promoter driving the KanR gene; the next 90 bp corresponding with part of the T1 and T2 terminators from the pDONR2.1 plasmid used as the bacterial plasmid backbone; and the last 70 bp derived from the DHFR-TS 3'UTR. The complete sequence and annotation is provided in Fig. S2. This data indicated that dramatic rearrangements have occurred at the site of plasmid integration. Taken together, we mapped the exact insertion site between nucleotide position 78952 and 78953 on chromosome V, in the promoter of gene 77.m00088 (Fig. 3E) and we detected irregularities suggestive of rearrangements at the 5'-end of the insertion site in the genome.

The protein encoded by gene 77.m00088 is highly conserved across evolution and is part of the eukaryotic type II chaperonin family. The type II chaperonins are cytoplasmic hetero-oligomeric protein complexes forming a ring structure named the TCP-1 ring complex or TRiC (TCP-1 stands for Tailless Complex Polypeptide 1) [24,25]. Two rings form a mature chaperonin to form a cavity wherein non-native proteins are folded correctly driven by ATP hydrolysis. The TRiC is composed of eight different but paralogous subunits called CCTs, which stands for chaperonin containing TCP1. The *Toxoplasma* gene we identified is an ortholog of subunit CCT θ , known as CCT8 in *Saccharomyces cerevisiae*. TgCCT θ shows 17.9% homology and 42.5% identity with human CCT θ (GenBank acc. no. NP.006576.2). Expression of YFP tagged CCT θ plasmids

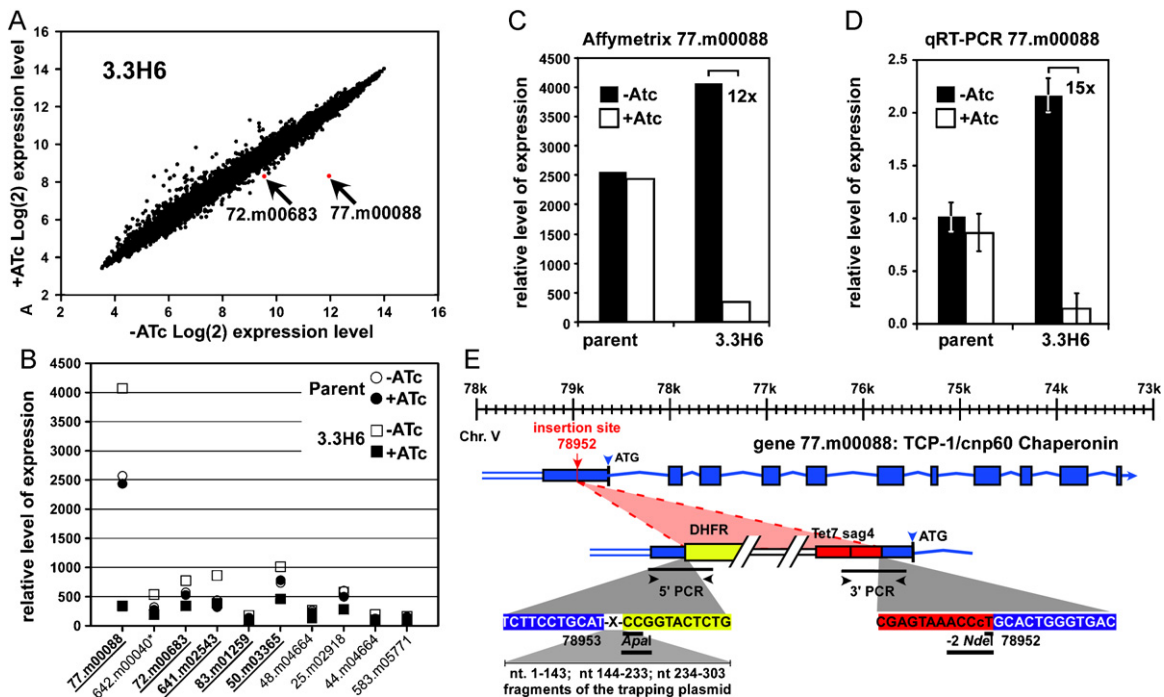


Fig. 4. Identification and mapping of the trapped gene in mutant 3.3H6. (A) Affymetrix chip expression by expression profiling of mutant 3.3H6 with or without 33 h of ATc induction: gene 77.m00088 displays the highest differential expression. (B) Overview of the top 10 genes with the highest relative differential expression pattern. The size of differential signal decreases from left to right. Data for parent and mutant 3.3H6 are shown. Underlined, bold gene names were validated by individual cosmid complementation (* 642.m00040 is not annotated as a gene anymore in the latest version of ToxoDB). (C) Affymetrix expression profiling detected a 12-fold ATc-dependent conditional expression of gene 77.m00088 in mutant 3.3H6, whereas no variation is detected in the parent. (D) By qRT-PCR a 15-fold ATc-dependent conditional expression of gene 77.m00088 is detected in mutant 3.3H6, whereas no variation is detected in the parent. Levels are relative to actin and data were averaged over five independent experiments; error bars denote standard error over five replicate experiments with $n = 3$ per experiment. (E) Schematic overview of the plasmid insertion breakpoints in gene 77.m00088 on chromosome V identified by PCR and sequencing. At the 5'-end breakpoint an unexpected 303 bp insertion was identified of which corresponds with three non-continuous fragments of the trapping plasmid. See [Supplementary Fig. S2](#) for the complete sequence and annotation.

in the parasite resulted in cytoplasmic localization (data not shown).

To validate whether CCT θ was responsible for the invasion and growth phenotype observed for mutant 3.3H6 we attempted to complement the mutant with a cosmid containing the wild-type allele of gene 77.m00088 [9]. Cosmid TOXO867 spans the entire genomic locus of CCT θ and was transfected into mutant 3.3H6. The integrity of cosmid TOXO867 was checked by restriction enzyme analysis (results not shown). Growth restoration was selected by growth in the presence of ATc. Unexpectedly, repeated attempts did not result in growth restoration. Subsequent attempts to complement with either N- or C-terminal YFP fusion plasmids of gene CCT θ driven by the constitutive α -tubulin promoter also did not result in growth restoration. The YFP signal in both cases localized to the cytoplasm when expressed in wild-type parasites (not shown). These results strongly suggest that CCT θ is not essential for the phenotype observed in mutant 3.3H6.

3.5. Identification of a suppressor in 3.3H6

The genomic insertion site of the trapping plasmid in gene 77.m00088 suggests rearrangements at the insertion site providing evidence for three independent segments on the insertional plasmid. These results could hint at tandem plasmid integrations. We sought to find additional evidence for potential rearrangement by Southern blotting. Fig. 5A shows a genetic map based on the sequence data at the 5'- and 3'-flanks for the insertion, compared to the wild-type locus. Restriction enzymes were selected to highlight the flanks as well as the structure of the inserting plasmid. Corresponding probes were designed on both flanks of the plasmid insertion (5'- and 3'-probe) as well as within the plasmid (KAN probe). As shown in Fig. 5B, the DNA fragment sizes match

the predicted sizes with exception of the 5'-probe/*AgeI* combination. The ~7 kb size of the observed band was significantly larger than the expected 4.6 kb band. This suggests additional insertions and/or rearrangements took place at the 5'-end of the inserting plasmid outside the region amplified by PCR to map the breakpoint (Fig. 4E). The KAN probe, detecting the insertional plasmid, showed a more complex profile, which dependent on the restriction enzyme, showed either 2 or 3 bands. Regardless of the restriction enzyme, the expected band was detected in all cases. One of the additional bands across the three restriction enzymes closely matches a head-to-tail insertion as it matches the size of the full-length plasmid, 4906 bp after removal of the linker. The intensity of the band at this size in the *XmnI* digested appears to have double intensity which either reflects a multiple tandem, or more likely, reflects an independent insertion coincidentally generating an ~5 kb band upon *XmnI* digestion. Either way, this leaves at least one additional band with the KAN probe unaccounted for, which indicates an additional independent insertion event elsewhere in the genome. Taken together, the Southern blot data largely confirms the PCR mapping while also providing evidence for additional rearrangements at the 5-end of the 77.m00088 locus, a tandem insertion, as well as at least one additional and possibly two plasmid insertions elsewhere in the genome.

Additionally, independent trapping plasmid insertions suggest that one of these plasmids could have trapped and controlled expression of an essential gene in an ATc dependent fashion. To identify the essential gene responsible for the 3.3H6 phenotype we considered the 4 genes with the next highest differential expression levels (Fig. 4B). We selected cosmids spanning the wild-type loci of these 4 genes and attempted to complement the growth phenotype of mutant 3.3H6 with these individual cosmids under ATc selection. Cosmid PSBLV88 spanning gene 72.m00683 did confer

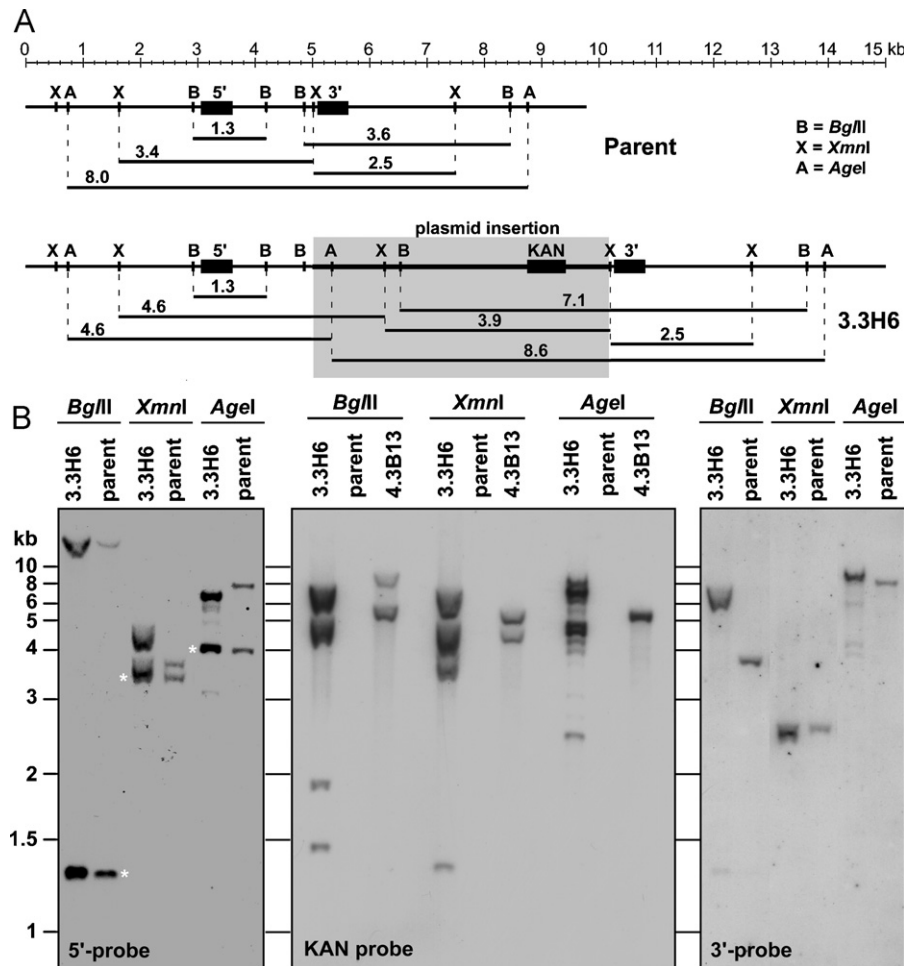


Fig. 5. Characterization of gene 77.m00088 and the Tet7sag4 insertion in mutant 3.3H6 by Southern blot. (A) Schematic of the 77.m00088 locus in wild-type and mutant 3.3H6 genomes. Plasmid insertion represented by grey-shaded box. Restriction sites of *Bgl*II, *Xmn*I and *Age*I used for the Southern blots are indicated with the expected restriction fragment sizes. Probe localizations are indicated by black boxes. (B) Southern blots hybridized with the 5'-probe, the KAN probe and the 3'-probe as indicated. Mutant 4.3B13 is included in the KAN probe hybridization. The 5'-probe cross-reacts with another, unknown fragment in the genome (bands marked with asterisk). The KAN probe demonstrates at least 2, but possibly 3, independent insertions in 3.3H6, whereas 2 insertions are detected in 4.3B13. The *Age*I fragment recognized by the 5'-probe in the 3.3H6 mutant is approximately 3 kb longer than expected; all other band sizes are as expected.

growth restoration, strongly suggesting this gene is responsible for the 3.3H6 phenotype. This gene only shows a 2.3-fold differential expression level in response to ATc with very low absolute expression levels (Fig. 6A). Confirmation that this locus is indeed able to restore growth was provided by two additional cosmids PSBM403 and PSBM924 spanning 72.m00683, which both conferred growth restoration (Fig. 6B). In addition, we used a PCR amplified genomic region spanning the 72.m00683 ORF and its promoter, which also conferred growth restoration as shown by growth curves (Fig. 6C). Subsequently, we tried mapping the insertion site by overlapping PCR primer pairs, which amplify 1–2 kb fragments from wild-type genomic DNA (Fig. 6B). However, if the 5 kb insertional plasmid inserted in the region spanned by the primer pair, then no product or a much larger product would be expected which would indicate the location of the plasmid insertion site. We tested a region spanning the two adjacent genes, but all primer pairs amplified in amplification of bands consistent with the wild-type locus in both the parent and mutant line (Fig. 6D). These results suggest that gene 72.m00683 acts as a suppressor of the 3.3H6 phenotype. In general, suppressors work by bypassing the actual mutated gene or pathway by overexpression of the suppressor gene. We have not formally assessed whether this applies to 72.m00683.

Gene 72.m00683 is annotated as a hypothetical protein of 187 amino acids and is also present in *N. caninum*. Otherwise this gene

is not conserved and provides no significant hits when BLASTP searched against the NCBI Nr database. In addition, no conserved domains were identified for this open reading frame when searched against the Pfam and SMART databases. Expression of a YFP-tagged 72.m00683 gene resulted in co-localization with a red fluorescent histone 2b fusion protein reporter in the nucleus (Fig. 6E). The YFP-tagged gene was able to functionally restore growth of mutant 3.3H6 under ATc indicating nuclear localization of the YFP-tagged gene is functional.

3.6. Identification of TAF250 as the gene responsible for the 4.3B13 defect

Gene expression profiling of mutant 4.3B13 identified gene 64.m00349 with a 9.4-fold reduction expression as the strongest candidate to be trapped by the Tet7sag4 promoter (Fig. 7A). We used cosmid complementation to validate whether this gene was responsible for the growth defect. Transfection of cosmid TOXOI78 spanning the wild-type locus of gene 64.m00349 into mutant 4.3B13 provided robust growth restoration under ATc (Fig. 7B). Cosmid TOXOI78 contains a 38 kb insert and includes one complete gene (64.m00350) and one partial gene (64.m00351), both upstream of 64.m00349. No complementation was observed using an unrelated cosmid. Subsequently, we designed a series of five

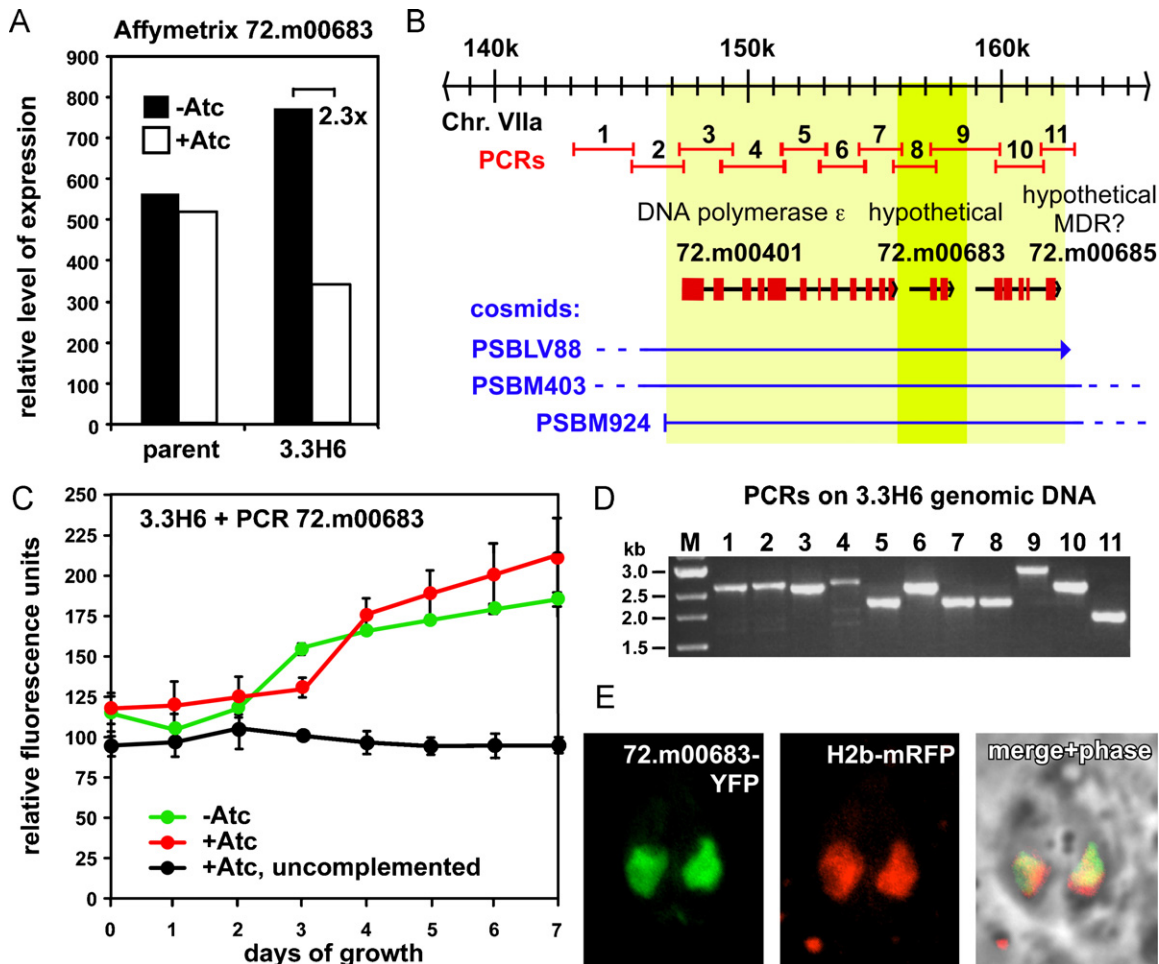


Fig. 6. Identification of gene 72.m00683 as a suppressor of mutant 3.3H6. (A) Affymetrix expression profiling detected a 2.3-fold ATc-dependent conditional expression of gene 72.m00683 in mutant 3.3H6, whereas no variation is detected in the parent. (B) Schematic overview of chromosome VIIa region containing gene 72.m00683. Three cosmids spanning gene 72.m00683 were used to validate its complementation competence, narrowing down the region of interest to the light yellow box. Subsequent PCR amplification of the genomic region marked by the dark yellow box restricted the region to only gene 72.m00683. In red 11 different primer pairs are indicated that were used to map the site of the trapping plasmid insertion. (C) Growth curve of mutant 3.3H6 stably complemented with gene 72.m00683 showing growth restoration in the presence of ATc (red line). Un-induced complemented (green line) and uncomplemented with ATc (black line) are included as well. (D) PCR products with the 11 primer pairs indicated in panel B show that all amplify the band sizes corresponding with the genomic locus. As such, no trapping plasmid insertion could be detected. (E) Expression of a tubulin promoter driven C-terminal YFP fusion of gene 72.m00683 co-transfected with a H2b-mRFP fusion proteins identifies nuclear localization. (For interpretation of the references to color in this figure legend, the reader is referred to the web version of the article.)

overlapping primer pairs to amplify 1–2 kb sections around the annotated translational start site of gene 64.m00349 to map the insertion site (Fig. 7C). We were unable to obtain a PCR product using primer pair 5 from mutant 4.3B13, whereas a robust product was obtained from the parent line (Fig. 7D). Subsequent fine mapping of the insertion site using the Tet7sag4 sense and DHFR anti-sense primer in combination with the primer pair 5 reverse and forward primers, respectively, resulted in strong PCR products. Sequencing of these products identified the 5'- and 3'-breakpoints between chromosome and plasmid (Fig. 7C). In this case, plasmid insertion resulted in a 2 bp deletion in the chromosome. On the 3'-end of the insertion a 7 bp deletion from the plasmid was mapped. At the 5'-end we again detected abnormalities, in this case a 999 bp insertion consisting of 82 bp encoding part of the kanamycin resistance gene followed by an 11 nucleotide composed mostly of cytosidine residues and finally 906 bp encoding a central part of the DHFR-TS cDNA, in opposite orientation. The complete inserted sequence and annotation is provided in Fig. S3. The plasmid insertion within the 64.m00349 gene is not in front of the predicted ATG start codon suggesting that this is not the start codon being used in the insertional mutant. However, four alternative in-frame ATG codons are present within the first

exon behind the insertion site and could function as *de facto* start codons (Fig. 7C). Gene 64.m00349 encodes a 2648 amino acid open reading frame and is annotated as a bromodomain-containing protein. Further sequence analysis and database searching revealed this gene is highly conserved. As recently reported, this gene is the most likely candidate for the TAF250 ortholog [26], which is a subunit of the RNA polymerase II TFIID protein complex [27]. Reciprocal BLASTP searches of ToxoDB with the human TAF250 orthologs (isoforms a, b, c, d, and e; GenBank acc. no. EAX05291.1, EAX05292.1, EAX05293.1, EAX05294.1, EAX05295.1, respectively) identifies gene 64.m00349 as the top hit (e−18 P-value). Phylogenetic analysis of TAF250 orthologs of various Apicomplexa and other eukaryotes shows clustering of the Apicomplexa species with very high bootstrap support (Fig. 7E). Overall, the tree branches with high bootstrap values along the expected eukaryotic lineage relations.

4. Discussion

We successfully developed a system to generate conditional mutants by random gene trapping and promoter replacement with a tetracycline regulatable promoter (Figs. 1 and 2). The two mutants

our understanding of the underlying rearrangement mechanisms in *Toxoplasma*.

In mutant 3.3H6 we mapped a conditional CCT θ allele, a component of the CCT chaperonin protein folding machinery. The best-studied *in vivo* substrates of CCT are actin and tubulin [39,40]. Not surprisingly, defects in these proteins lead to cell cycle arrests and cytoskeleton deformations [25,40]. *Toxoplasma* cell division requires microtubules, whereas host cell invasion requires actin to support motility as well as an intact cytoskeleton containing microtubules [41,42]. As such, the cell division and invasion phenotype of mutant 3.3H6 is consistent with this mutation (Fig. 3). However, our complementation efforts of mutant 3.3H6 with various CCT θ constructs did not result in restoration of the wild-type phenotype. The same validation approaches tried here were effective in complementing and validating candidate genes in over two dozen temperature sensitive mutants [9] and therefore it is unlikely the conditional CCT θ allele is responsible for the 3.3H6 invasion and growth defect. Most likely another gene is trapped in mutant 3.3H6, which is essential. In this case, the CCT θ reduction in expression is likely not zero, and enough protein is present to allow proper protein folding to a level enough to sustain viability. Since we demonstrated more than one plasmid insertion in the genomic DNA of mutant 3.3H6 (Fig. 5), a second trapped locus of an essential gene is the most logical explanation of the data. Efforts to map this second locus did not identify the trapped locus but identified a suppressor of the phenotype which expression was conditional upon ATc (Fig. 6). The identified gene is unique to *Toxoplasma* and *Neospora* whereas no functional domains could be identified. We did demonstrate the gene product localizes to the nucleus (Fig. 6E). How the suppressor gene contributes to the phenotype cannot be deduced from the available data.

The bromodomain containing protein identified in mutant 4.3B13 was indeed ATc conditional and responsible for the observed phenotype (Fig. 7). This protein is the *Toxoplasma* ortholog of TAF250 [26], a component of the TFIID component of the RNA polymerase II complex and is involved in DNA recognition [27,43]. As such, the growth phenotype of mutant 4.3B13 is likely very basal due to a defect in transcription. The modest invasion defect is probably a secondary effect that originates in a more general transcriptional defect (Fig. 3A). The absence of an arrest at a particular stage in development (Fig. 3I) or the cell cycle (Fig. 3D) are consistent with a defect in a basic mechanism such as transcription which is crucial at all stages of the cell cycle.

Taken together, we established a forward genetic method to generate conditional mutants by insertional mutagenesis that expands the genetic toolbox available for *Toxoplasma*. However, when the low incidence of mutant isolation is offset against other methods to generate mutants and when also taking into account that the trapped gene should be compatible with the Tet-promoter, the method described here would not be the first choice. Furthermore we demonstrated that genome-wide expression profiling is an excellent tool to map the insertional events due to the conditional gene transcription of the mutants. Analysis of the insertional breakpoints provides evidence for rearrangements that explain the generally low efficiencies seen to map insertional events in *T. gondii*. Finally, the identification of TAF250 as the conditional gene in mutant 4.3B13 demonstrates TAF250 is essential for *T. gondii* growth. This parasite mutant provides a great tool to study transcription, which will be the focus of future experiments.

Acknowledgements

Mutants were originally generated in the lab of Dr. Boris Striepen, University of Georgia. We are grateful to Nico Boot for assistance with plasmid cloning, and Dr. William Sullivan Jr. for useful discussion.

This work was supported by an American Heart Association Scientist Development Grant to MJG (0635480N) and the following NIH grants: AI028724 (DSR), AI077268 and RR016469 (PHD).

Appendix A. Supplementary data

Supplementary data associated with this article can be found, in the online version, at doi:10.1016/j.molbiopara.2010.10.007.

References

- [1] Montoya JG, Liesenfeld O. Toxoplasmosis. *Lancet* 2004;363:1965–76.
- [2] Gubbels MJ, White M, Szatanek T. The cell cycle and *Toxoplasma gondii* cell division: tightly knit or loosely stitched? *Int J Parasitol* 2008;38:1343–58.
- [3] Striepen B, Jordan CN, Reiff S, van Dooren GG. Building the perfect parasite: cell division in apicomplexa. *PLoS Pathog* 2007;3:e78.
- [4] White MW, Radke J, Conde de Felipe M, Lehmann M. Cell cycle control/parasite division. Norwich, UK: Horizon Scientific Press; 2007.
- [5] Meissner M, Schluter D, Soldati D. Role of *Toxoplasma gondii* myosin A in powering parasite gliding and host cell invasion. *Science* 2002;298:837–40.
- [6] Meissner M, Brecht S, Bujard H, Soldati D. Modulation of myosin A expression by a newly established tetracycline repressor-based inducible system in *Toxoplasma gondii*. *Nucleic Acids Res* 2001;29:E115.
- [7] van Poppel NF, Welagen J, Duisters RF, Vermeulen AN, Schaap D. Tight control of transcription in *Toxoplasma gondii* using an alternative tet repressor. *Int J Parasitol* 2006.
- [8] Herm-Gotz A, Agop-Nersesian C, Munter S, et al. Rapid control of protein level in the apicomplexan *Toxoplasma gondii*. *Nat Methods* 2007;4:1003–5.
- [9] Gubbels MJ, Lehmann M, Muthalagi M, et al. Forward genetic analysis of the apicomplexan cell division cycle in *Toxoplasma gondii*. *PLoS Pathog* 2008;4:e36.
- [10] Knoll LJ, Furie GL, Boothroyd JC. Adaptation of signature-tagged mutagenesis for *Toxoplasma gondii*: a negative screening strategy to isolate genes that are essential in restrictive growth conditions. *Mol Biochem Parasitol* 2001;116:11–6.
- [11] Roos DS, Donald RG, Morrisette NS, Moulton AL. Molecular tools for genetic dissection of the protozoan parasite *Toxoplasma gondii*. *Methods Cell Biol* 1994;45:27–63.
- [12] Gubbels MJ, Li C, Striepen B. High-throughput growth assay for *Toxoplasma gondii* using yellow fluorescent protein. *Antimicrob Agents Chemother* 2003;47:309–16.
- [13] Gubbels MJ, Vaishnav S, Boot N, Dubremetz JF, Striepen B. A MORN-repeat protein is a dynamic component of the *Toxoplasma gondii* cell division apparatus. *J Cell Sci* 2006;119:2236–45.
- [14] Striepen B, White MW, Li C, et al. Genetic complementation in apicomplexan parasites. *Proc Natl Acad Sci USA* 2002;99:6304–9.
- [15] Carey KL, Westwood NJ, Mitchison TJ, Ward GE. A small-molecule approach to studying invasive mechanisms of *Toxoplasma gondii*. *Proc Natl Acad Sci USA* 2004;101:7433–8.
- [16] Lorestani A, Sheiner L, Yang K, Robertson SD, Sahoo N, Brooks CF, Ferguson DJP, Striepen B, Gubbels M-J. A *Toxoplasma* MORN1 null mutant is defective in basal complex assembly and apicoplast division. *PLoS ONE* 2010;5:e12302.
- [17] Anderson-White BR, Ivey FD, Cheng K, Szatanek T, Lorestani A, Beckers CJ, Ferguson DJP, Sahoo N, Gubbels MJ. A family of intermediate filament-like proteins is sequentially assembled into the cytoskeletal scaffold of *Toxoplasma gondii*. *Cell Microbiol*; in press, doi:10.1111/j.1462-5822.2010.01514.x.
- [18] Behnke MS, Radke JB, Smith AT, Sullivan Jr WJ, White MW. The transcription of bradyzoite genes in *Toxoplasma gondii* is controlled by autonomous promoter elements. *Mol Microbiol* 2008;68:1502–18.
- [19] Larkin MA, Blackshields G, Brown NP, et al. Clustal W and Clustal X version 2.0. *Bioinformatics* 2007;23:2947–8.
- [20] Tamura K, Dudley J, Nei M, Kumar S. MEGA4: Molecular Evolutionary Genetics Analysis (MEGA) software version 4.0. *Mol Biol Evol* 2007;24:1596–9.
- [21] Donald RG, Roos DS. Stable molecular transformation of *Toxoplasma gondii*: a selectable dihydrofolate reductase–thymidylate synthase marker based on drug-resistance mutations in malaria. *Proc Natl Acad Sci USA* 1993;90:11703–7.
- [22] Radke JR, Striepen B, Guerini MN, Jerome ME, Roos DS, White MW. Defining the cell cycle for the tachyzoite stage of *Toxoplasma gondii*. *Mol Biochem Parasitol* 2001;115:165–75.
- [23] Nishi M, Hu K, Murray JM, Roos DS. Organellar dynamics during the cell cycle of *Toxoplasma gondii*. *J Cell Sci* 2008;121:1559–68.
- [24] Spiess C, Meyer AS, Reissmann S, Frydman J. Mechanism of the eukaryotic chaperonin: protein folding in the chamber of secrets. *Trends Cell Biol* 2004;14:598–604.
- [25] Brackley KI, Grantham J. Activities of the chaperonin containing TCP-1 (CCT): implications for cell cycle progression and cytoskeletal organisation. *Cell Stress Chaperones* 2009;14:23–31.
- [26] Dixon SE, Stilger KL, Elias EV, Naguleswaran A, Sullivan Jr WJ. A decade of epigenetic research in *Toxoplasma gondii*. *Mol Biochem Parasitol* 2010;173:1–9.
- [27] Albright SR, Tjian R. TAFs revisited: more data reveal new twists and confirm old ideas. *Gene* 2000;242:1–13.

- [28] Bozdech Z, Llinas M, Pulliam BL, Wong ED, Zhu J, DeRisi JL. The transcriptome of the intraerythrocytic developmental cycle of *Plasmodium falciparum*. *PLoS Biol* 2003;1:E5.
- [29] Le Roch KG, Zhou Y, Blair PL, et al. Discovery of gene function by expression profiling of the malaria parasite life cycle. *Science* 2003;301:1503–8.
- [30] Behnke MS, Wootton JC, Lehmann MM, Radke JB, Lucas O, Nawas J, Sibley LD, White MW. Coordinated progression through two subtranscriptomes underlies the tachyzoite cycle of *Toxoplasma gondii*. *PLoS One* 2010;5:e12354.
- [31] McAleer MA, Coffey AJ, Dunham I. DNA rescue by the vectorette method. *Methods Mol Biol* 2003;226:393–400.
- [32] Li JL, Cox LS. Identification of an MCM4 homologue expressed specifically in the sexual stage of *Plasmodium falciparum*. *Int J Parasitol* 2001;31:1246–52.
- [33] Murry JP, Sasseti CM, Lane JM, Xie Z, Rubin EJ. Transposon site hybridization in *Mycobacterium tuberculosis*. *Methods Mol Biol* 2008;416:45–59.
- [34] Donald RG, Roos DS. Insertional mutagenesis and marker rescue in a protozoan parasite: cloning of the uracil phosphoribosyltransferase locus from *Toxoplasma gondii*. *Proc Natl Acad Sci USA* 1995;92:5749–53.
- [35] Frankel MB, Mordue DG, Knoll LJ. Discovery of parasite virulence genes reveals a unique regulator of chromosome condensation 1 ortholog critical for efficient nuclear trafficking. *Proc Natl Acad Sci USA* 2007;104:10181–6.
- [36] Arrizabalaga G, Ruiz F, Moreno S, Boothroyd JC. Ionophore-resistant mutant of *Toxoplasma gondii* reveals involvement of a sodium/hydrogen exchanger in calcium regulation. *J Cell Biol* 2004;165:653–62.
- [37] Hastings PJ, Lupski JR, Rosenberg SM, Ira G. Mechanisms of change in gene copy number. *Nat Rev Genet* 2009;10:551–64.
- [38] Quinlan AR, Clark RA, Sokolova S, et al. Genome-wide mapping and assembly of structural variant breakpoints in the mouse genome. *Genome Res* 2010;20:623–35.
- [39] Hynes G, Sutton CW, Willison USKR. Peptide mass fingerprinting of chaperonin-containing TCP-1 (CCT) and copurifying proteins. *FASEB J* 1996;10:137–47.
- [40] Ursic D, Sedbrook JC, Himmel KL, Culbertson MR. The essential yeast Tsp1 protein affects actin and microtubules. *Mol Biol Cell* 1994;5:1065–80.
- [41] Dobrowolski JM, Sibley LD. Toxoplasma invasion of mammalian cells is powered by the actin cytoskeleton of the parasite. *Cell* 1996;84:933–9.
- [42] Shaw MK, Compton HL, Roos DS, Tilney LG. Microtubules, but not actin filaments, drive daughter cell budding and cell division in *Toxoplasma gondii*. *J Cell Sci* 2000;113(Pt 7):1241–54.
- [43] Chalkley GE, Verrijzer CP. DNA binding site selection by RNA polymerase II TAFs: a TAF(II)250-TAF(II)150 complex recognizes the initiator. *EMBO J* 1999;18:4835–45.